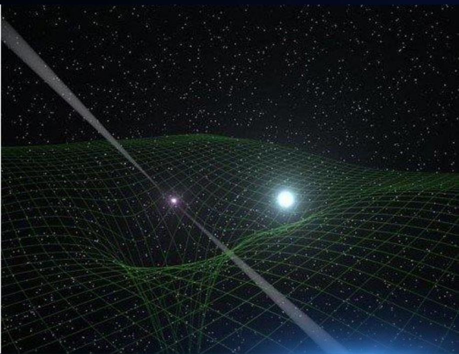 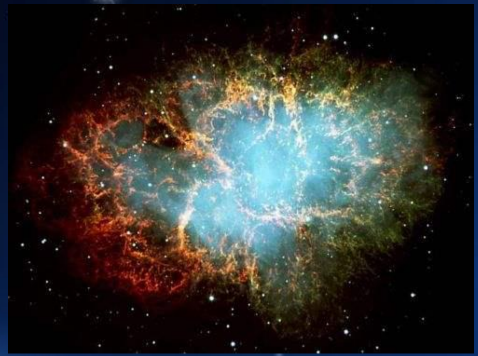 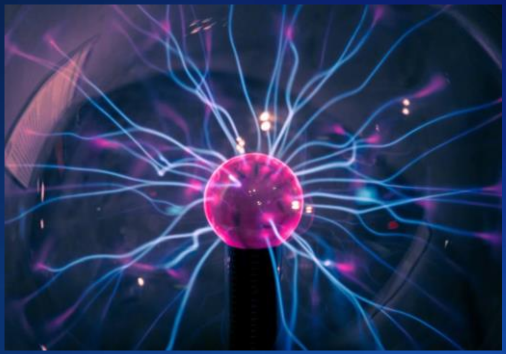 

Pulsar Giant Pulse:
Coherent instability at near light cylinder

Speaker：Weiyang Wang（王维扬）

NAOC

2018.7

CONTENTS

Pulse and GP

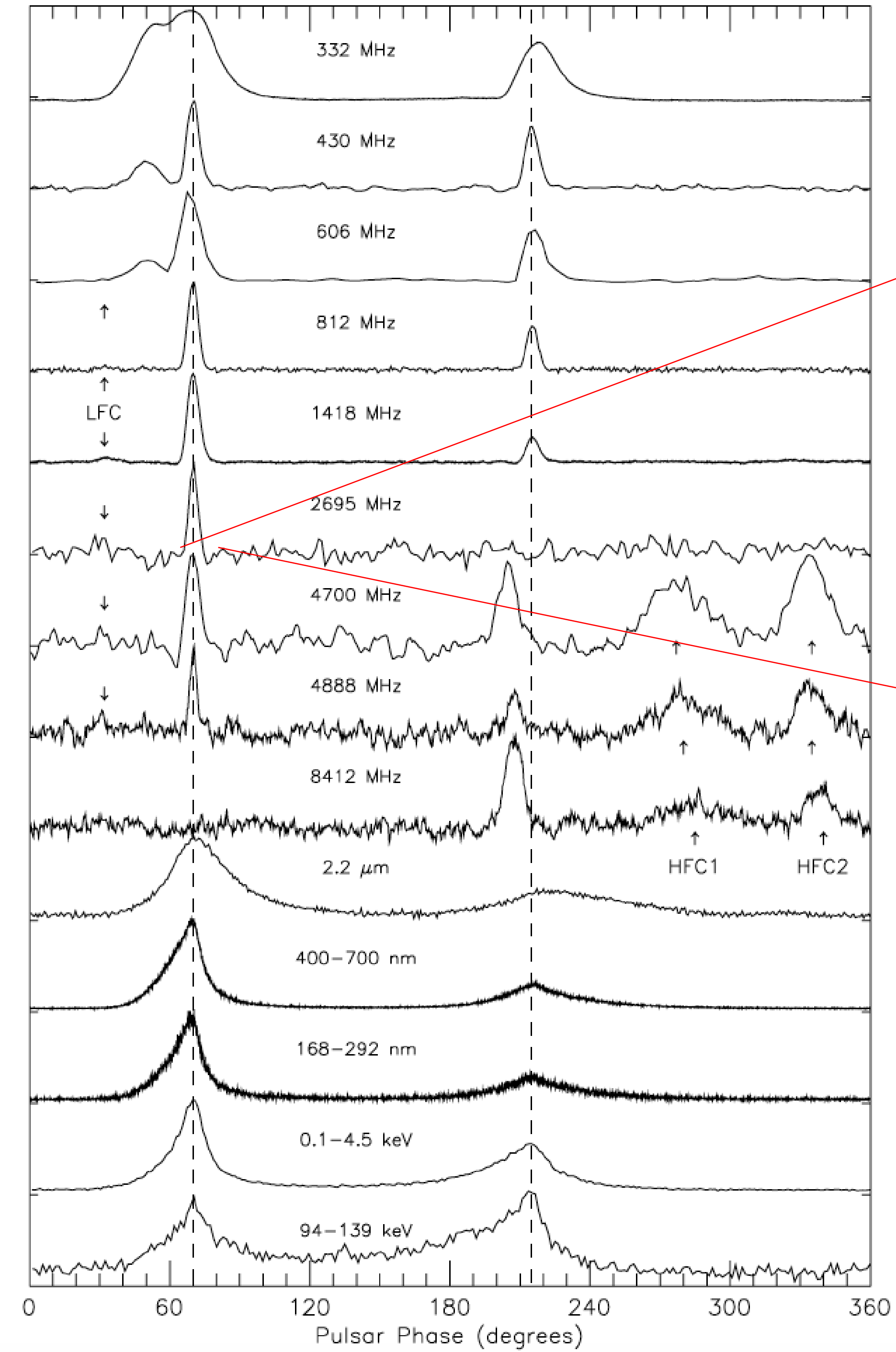

Pulses in the Crab pulsar

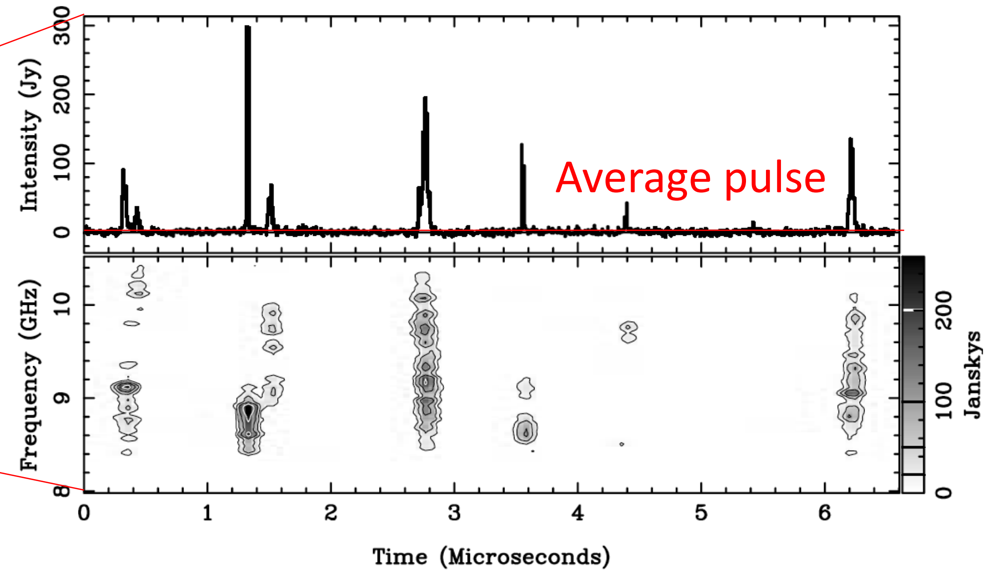

Some bright individual pulses are found. Their peak fluxes are tens of thousands of the mean profile.

e.g., Hankins & Eilek 2007

Properties of GP

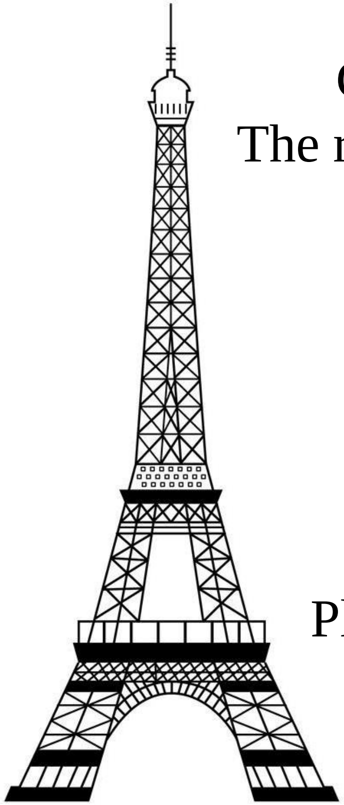

Giant pulse:
The real Eiffel Tower

Averaged pulse:
Plastic model sold in the Eiffel Tower

- Tens or hundreds, or even thousands or tens of thousands in individual cases.
- Short durations.
- High brightness temperature (e.g., 10^37 K).
- High linear or circular polarization.
- Power laws

Two types of GPs

Type I: $B_{LC} \approx 10^6$ G
Type II: $B_{LC} \approx 10 - 100$ G

PSR	P (s)	Frequency (MHz)	B_{LC} (G)	S_{GP}/S_{avg}	Reference
B0031−07	0.9430	40,111	6.87	400	Kuzmin & Ershov (2004)
J0218+4232	0.0023	610	3.14×10^5	-	Joshi et al. (2004)
B0301+19	1.3876	111	4.67	69	Kazantsev et al. (2017)
B0531+21	0.0334	20-15100	9.35×10^5	50000	Kostyuk et al. (2003); Jessner et al. (2010) Ellingson et al. (2013); Hankins et al. (2015)
B0540−69	0.0506	1380	3.53×10^5	5000	Johnston & Romani (2003)
B0643+80	1.2144	103	11.1	-	Malofeev et al. (1998)
B0656+14	0.3849	111	7.49	630	Kuzmin & Ershov (2006)
B0950+08	0.2531	39 − 112	138	490	Smirnova (2012); Tsai et al. (2015)
B1112+50	1.6564	111	4.15	80	Ershov & Kuzmin (2003)
B1133+16	1.1879	111	11.7	86	Kazantsev & Potapov (2015)
B1237+25	1.3824	111	4.05	65	Kazantsev & Potapov (2017)
J1752+2359	0.4091	111	69.6	320	Ershov & Kuzmin (2006)
B1820−30A	0.0054	6850	2.47×10^5	1700	Knight et al. (2005)
B1821−24	0.0031	1510	7.25×10^5	-	Romani & Johnston (2001)
B1937+21	0.0016	111-5500	9.93×10^5	600	Kuzmin & Losovsky (2002); Soglasnov et al. (2004)
B1957+20	0.0016	610	3.68×10^5	-	Joshi et al. (2004)

Here PSR is a pulsar name, P is period and S_{GP}/S_{avg} is an excess of the peak flux density of a strongest GP over the peak flux density of an AP.

P-dP/dt Diagram

Type I: $B_{LC} \sim 10^6$ G

Type II(Not so-giant): $B_{LC} \sim 10 - 100$ G

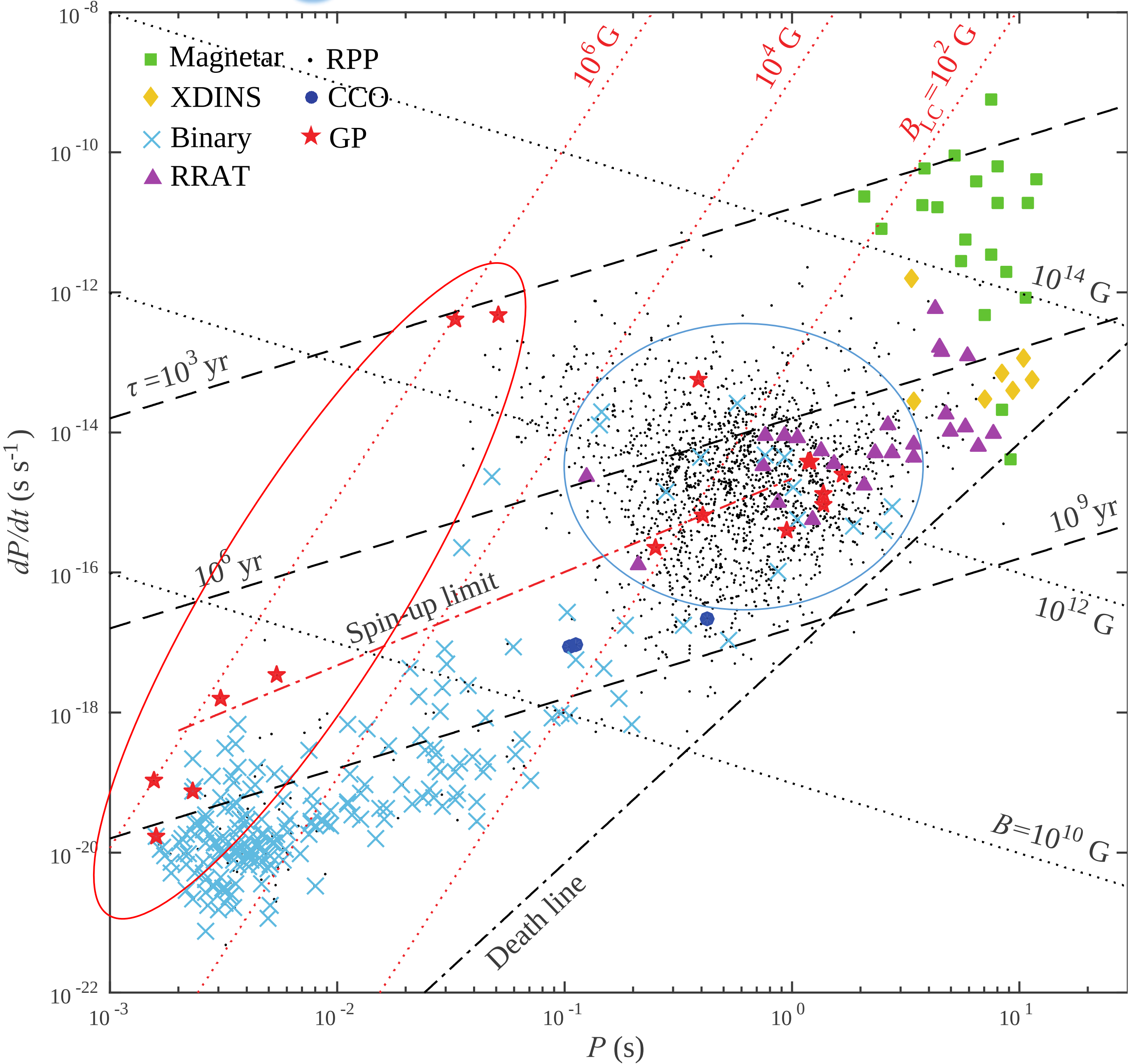

Type I GP with X-ray

For instance, in PSR J0218+4232, type I GPs are coincident with the phases of the X-ray peaks whereas deviates from peaks of mean radio pulse profile.

Pulse phases coincidence of radio GP and high energy emission is interpreted by their same emission area.

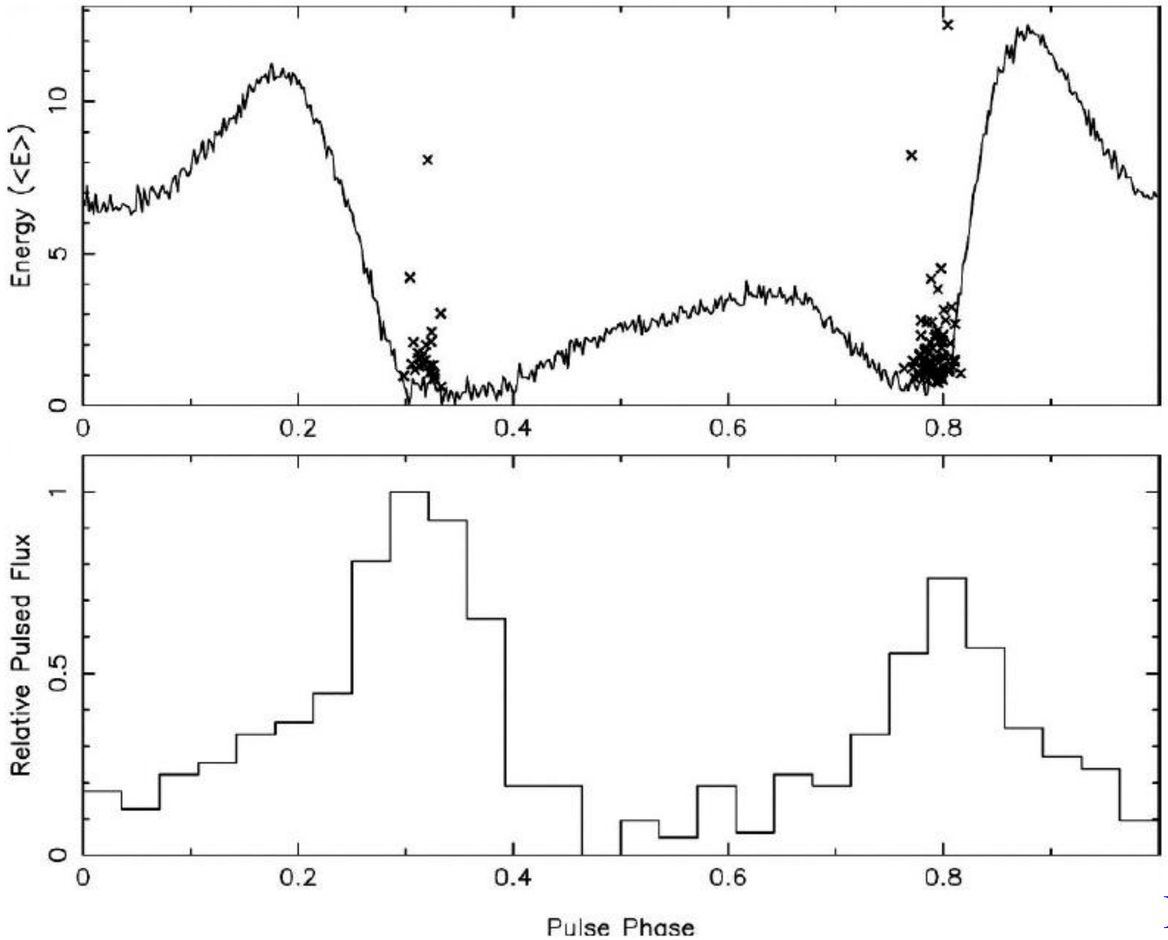

Knight et al. 2006

GP in the Crab pulsar

Main-pulse:

The temporal occurrence of GPs is random but at frequencies below 3 GHz they always occur at the phase of either the Crab pulsar's main pulse (MP) or interpulse (IP; Lundgren 1994).

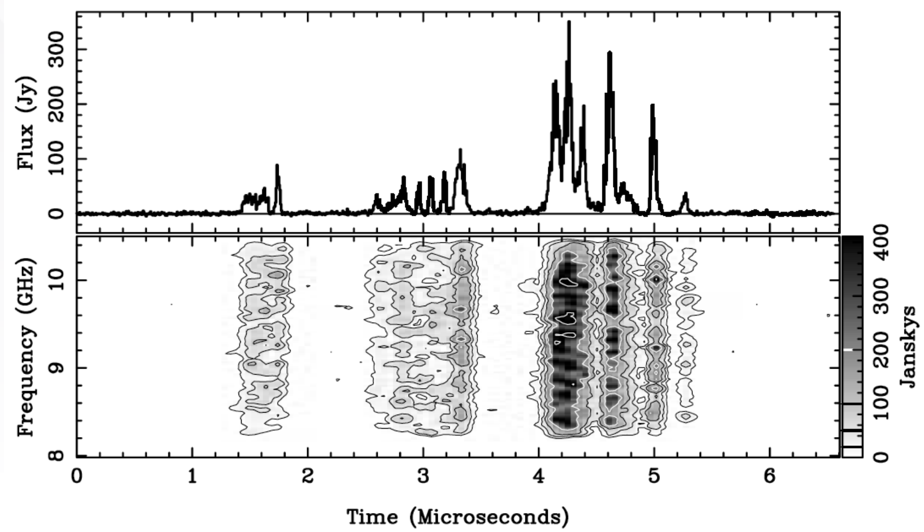

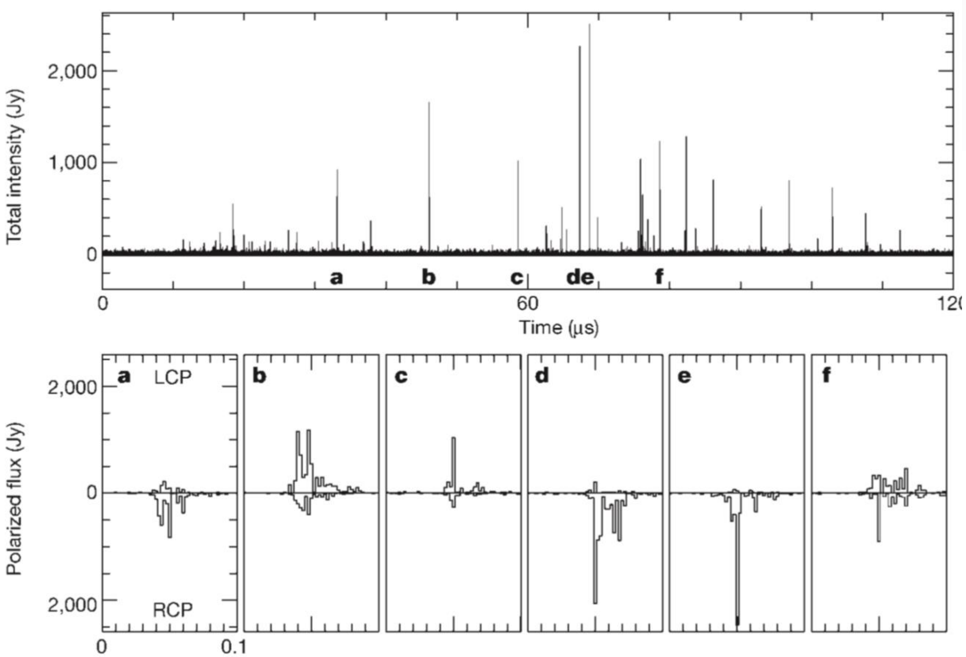

Most MPs consist of one to several microbursts; the brightest microburst in an MP can occur anywhere within the pulse average envelope. The microbursts can often be resolved into overlapping, short-lived "nanoshots." Polarization of the nanoshot is rapidly changing.

Hankins et al. 2003; Hankins & Eilek 2007

GP in the Crab pulsar

Inter-pulse:

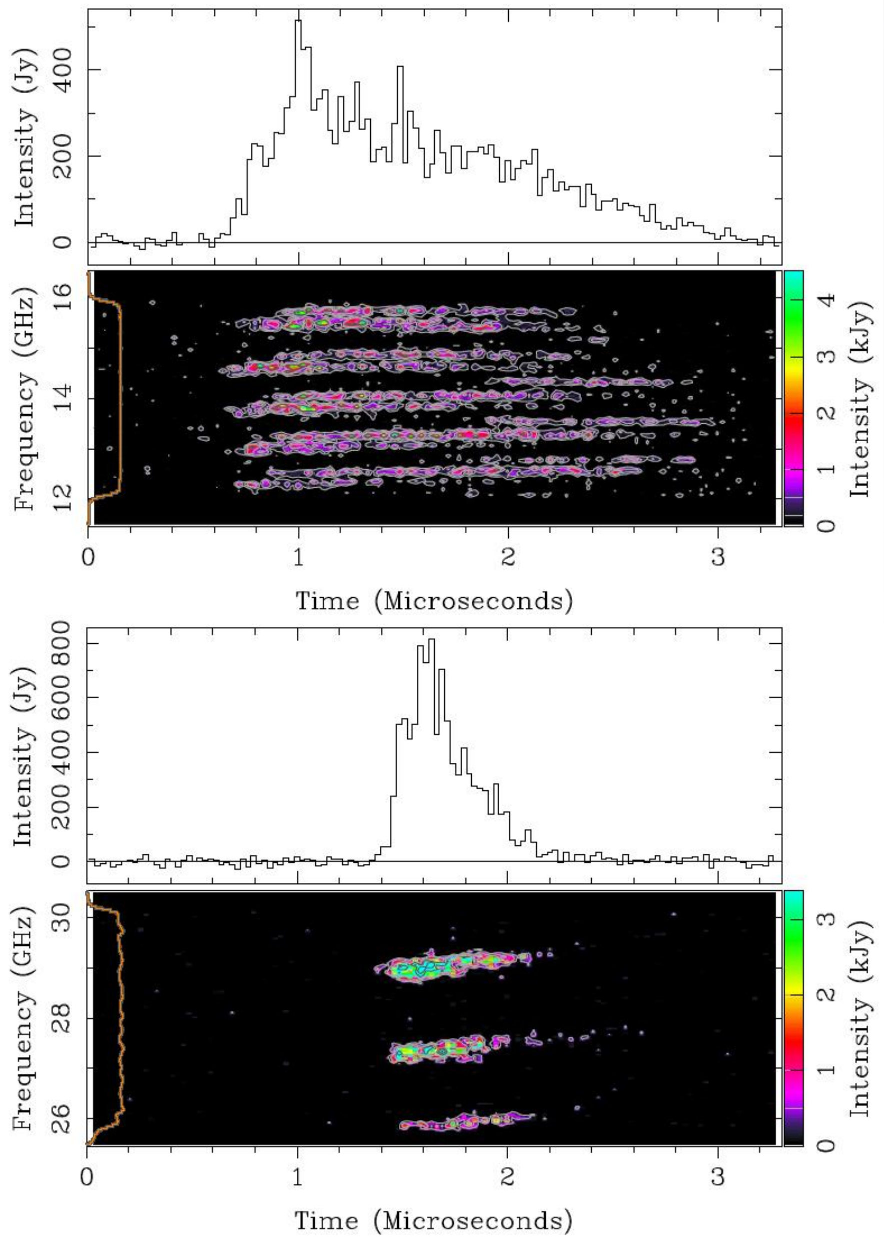

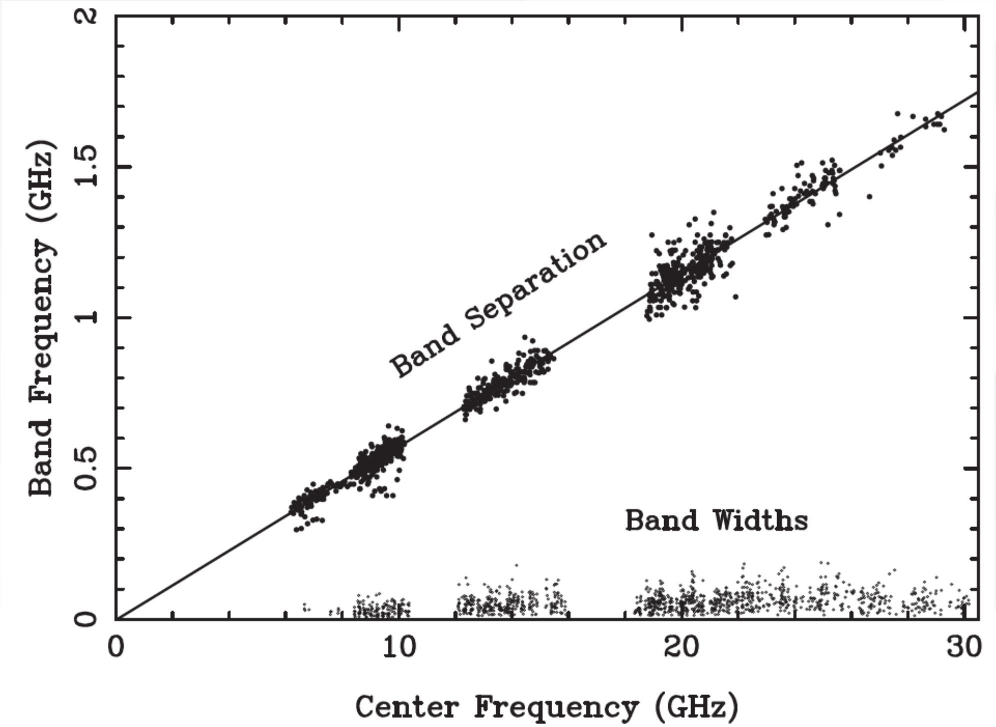

$$\Delta\nu = -0.0023 \pm 0.0030 + (0.0574 \pm 0.0002)\nu$$

$$\nu \propto \exp(-s) \quad ?!$$

Hankins et al. 2016

Emission Region of type I GP

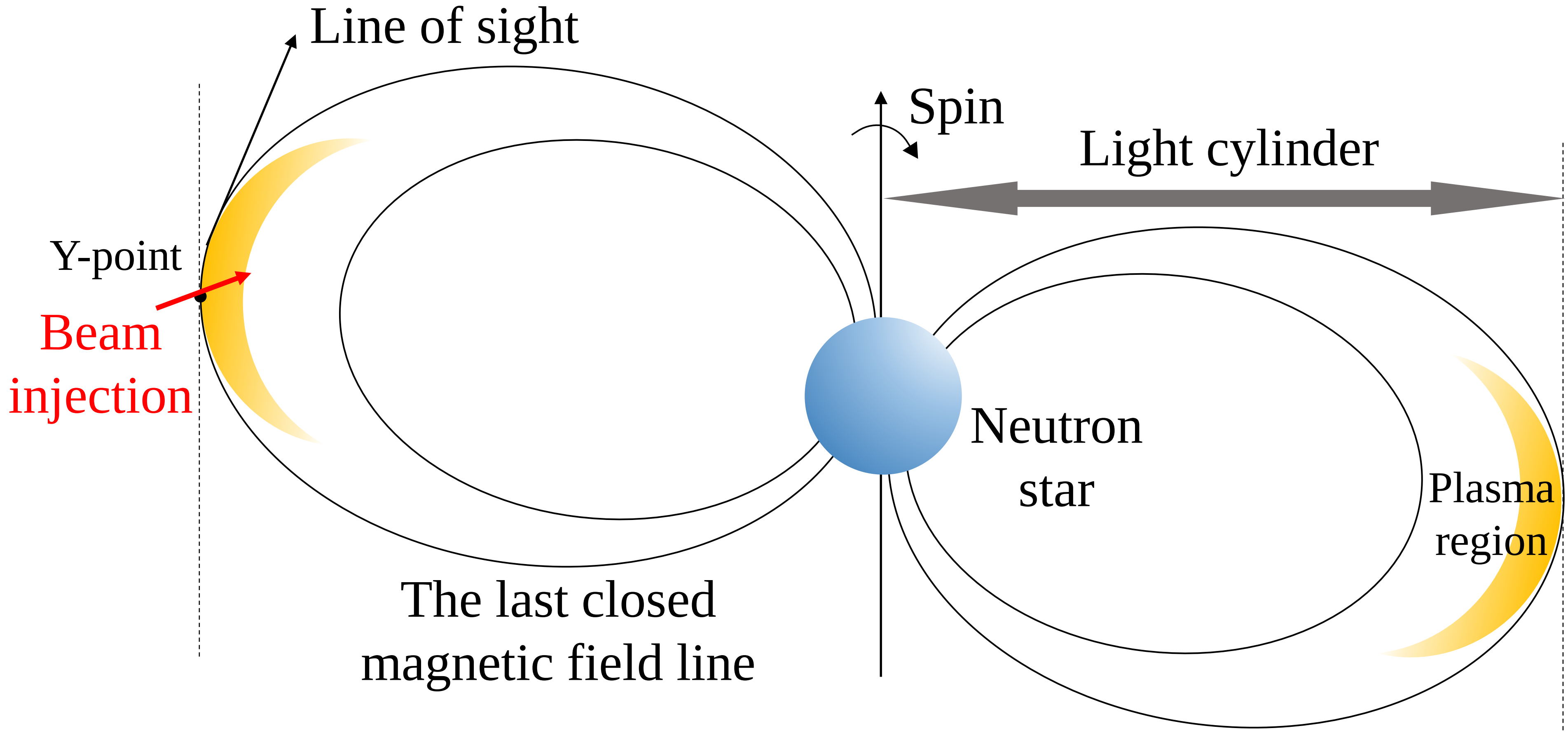

Magnetic reconnection occurs at near LC that generates electron−positron pair plasma injected into closed field line regions via the Y-point.

Cyclotron resonance instability

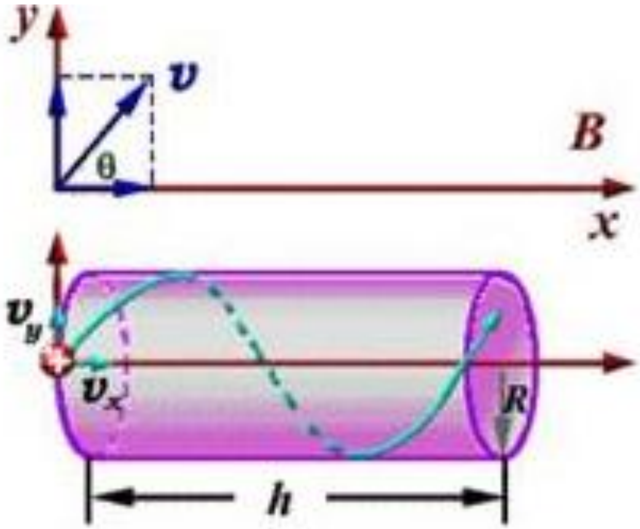

Wave-Particle resonance:

$$\omega - k_{\|} v_{\|} = s \frac{\omega_B}{\gamma_b}$$

Dispersion:

$$N_q^2 = \frac{k^2 c^2}{\omega^2} = 1 - \frac{\Omega_{p,b}^2}{\omega\left(\omega + \tau_q \Omega_B\right)},$$

$$\tau_q = -s_q + q\sqrt{s_q^2 + \cos^2\theta},$$

$$s_q = \frac{\omega \Omega_B \sin^2\theta}{2\left(\omega^2 - \Omega_{p,b}^2\right)},$$

Ultra-relativistic plasma

High magnetic field

The spectrum exhibits zebra pattern during the cyclotron instability occurs.

$$\omega = \frac{\Omega_{p,b}^2}{2s\Omega_{B,b}} \mp \Omega_{B,b}.$$

Cold Background resonance

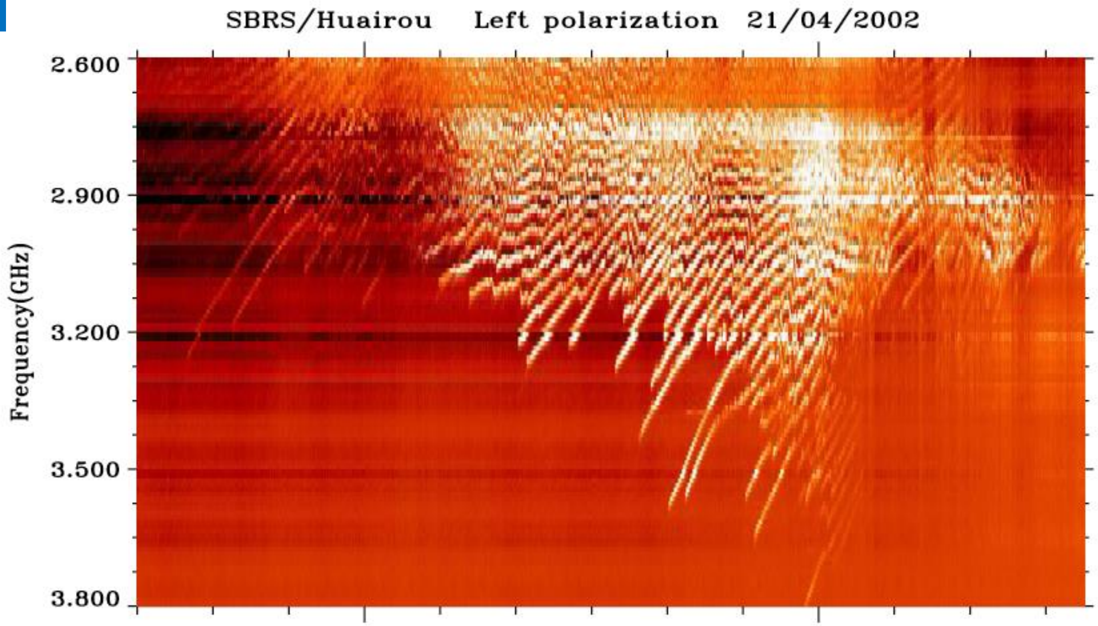

Double Plasma resonance in Solar Zebra pattern (Tan et al. 2014)

Resonance condition

$$\omega = \omega_{\rm uh} = \sqrt{\Omega_{p,c}^2 + \Omega_{B,c}^2},$$

The oscillation of background plasma frequency is the upper hybrid frequency.

$$\frac{\Omega_{p,c}(R+\Delta R)}{\omega_B(R+\Delta R)} \simeq \frac{\Omega_{p,c}(R)}{\omega_B(R)}[1-(\frac{1}{L_B}-\frac{1}{2L_n})\Delta R],$$

The stripe frequency separation is

$$\Delta\omega_{s,s+1} = \omega_s - \omega_{s+1} \simeq \frac{2\omega_s\omega_B}{\Omega_{p,c}\gamma_c\kappa(\frac{2L_n}{L_B}-1)}.$$

Coherent instability at near LC

Electron cyclotron

Cyclotron resonance

Generate Band structure

Excited cyclotron emission

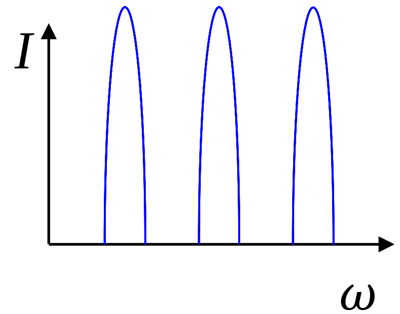

$$\Gamma_c \simeq \omega_B \gamma_0 \frac{n_b}{n_c} \left(\frac{\Omega_{p,b}}{\omega_B}\right)^4 \gamma_p^{-2} \gtrsim 10^2\,\mathrm{s}^{-1},$$

Background plasma resonance

Modulate band structure

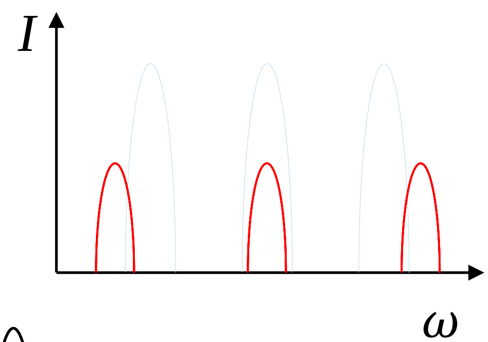

Coherent Emission

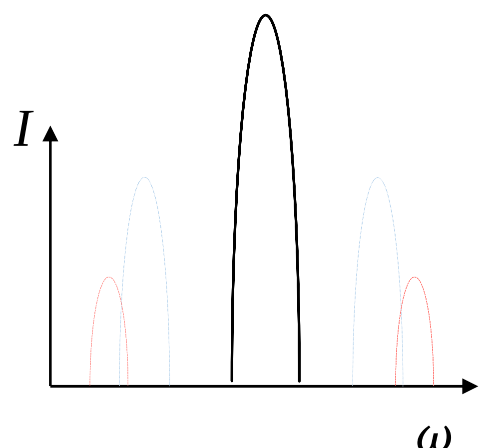

Band structure of the Crab Pulsar

$$\Delta\nu = -0.0023 \pm 0.0030 + (0.0574 \pm 0.0002)\nu$$

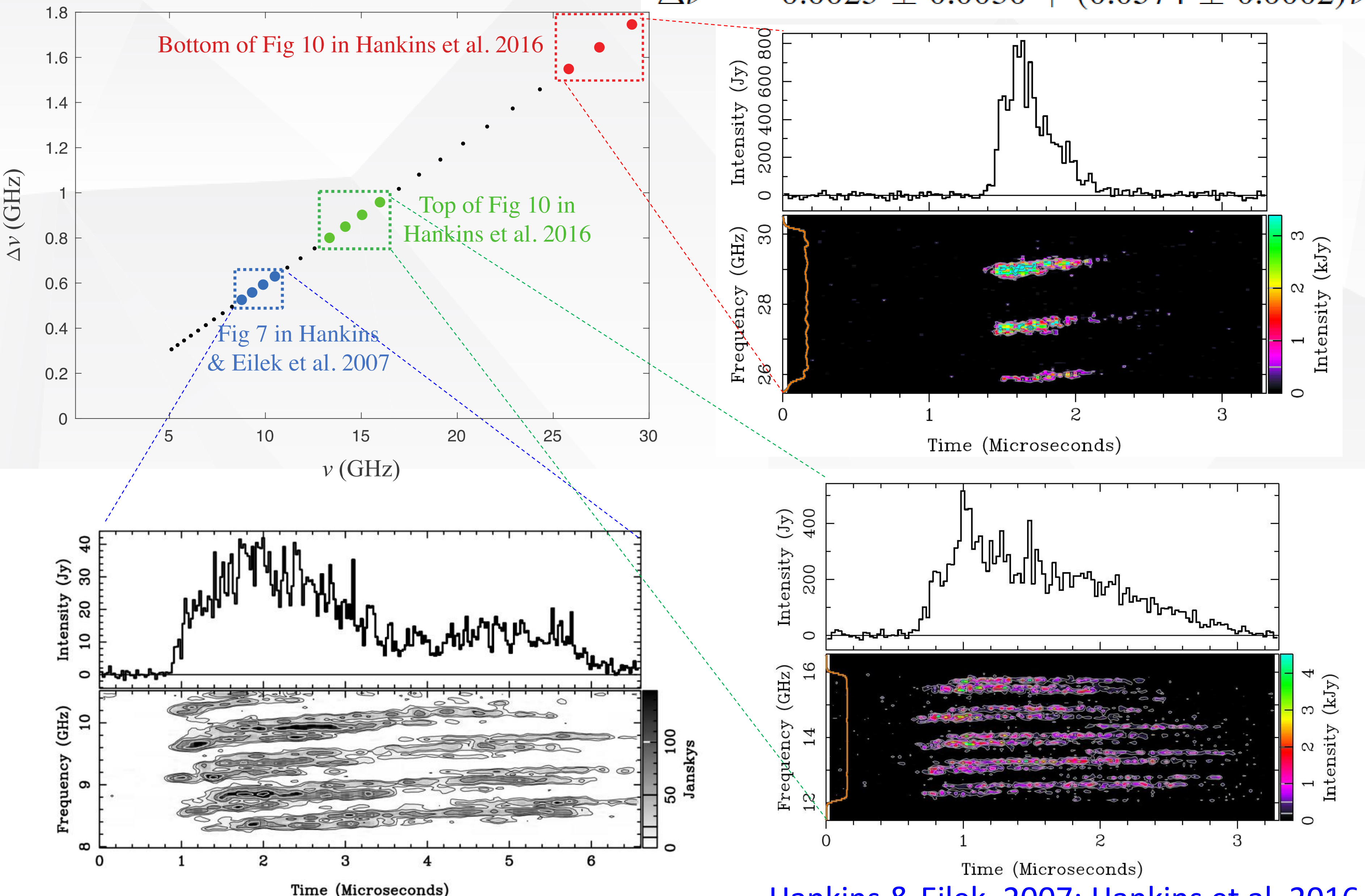

Hankins & Eilek, 2007; Hankins et al. 2016

Band structure of the Crab Pulsar

$$\Delta\omega_{s,s+1} = \omega_s - \omega_{s+1} \simeq \frac{2\omega_s\omega_B}{\Omega_{p,c}\gamma_c\kappa(\frac{2L_n}{L_B} - 1)}.$$

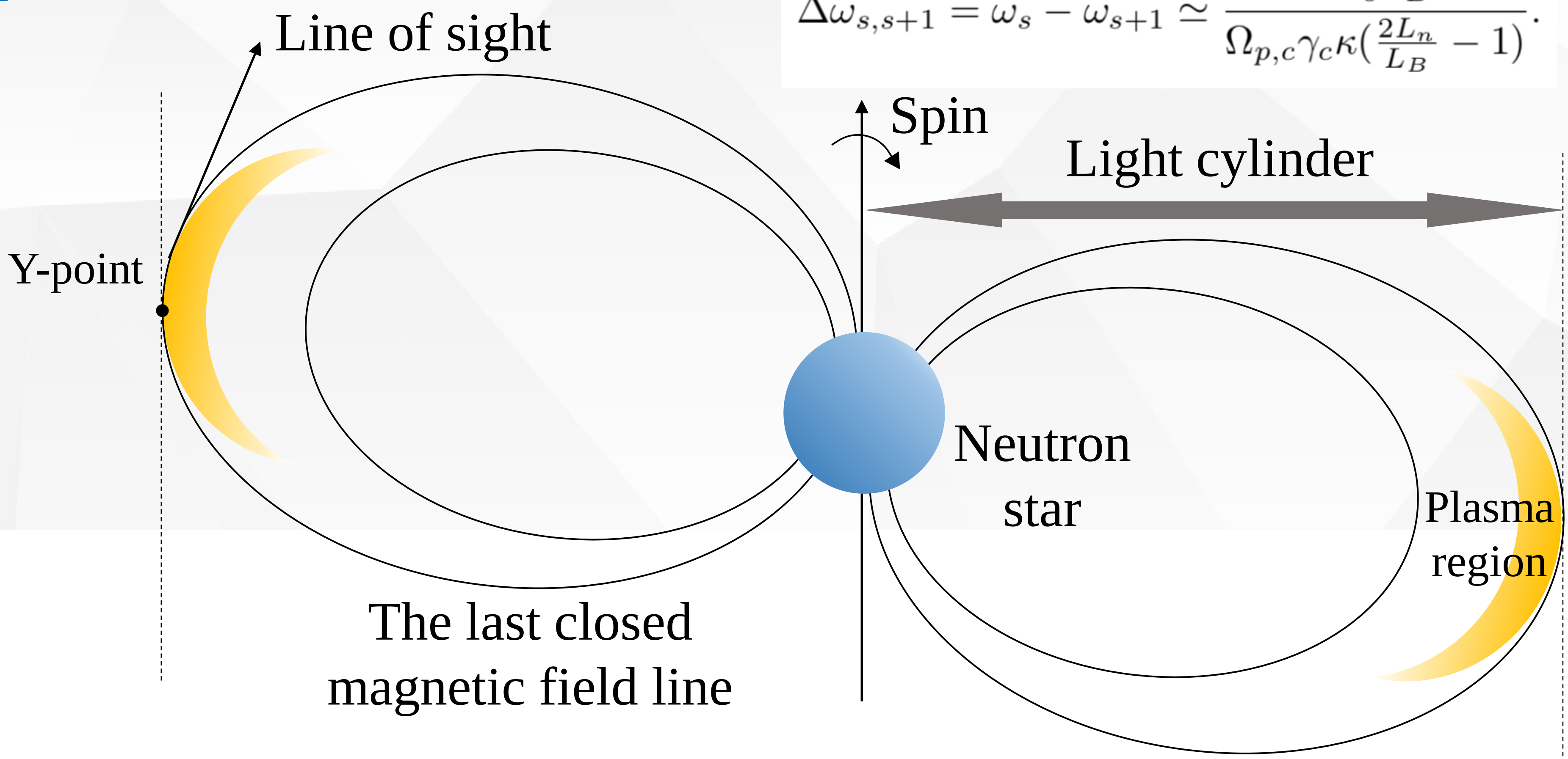

Beamed plasma: $n_b > 8.4 \times 10^{13}\ \mathrm{cm}^{-3}$, $\gamma_b \sim 10^6$

Background plasma: $n_c = 10^{13-15}\ \mathrm{cm}^{-3}, \gamma_c = 10^{2-4}$

Gradient: $\frac{dn_c}{dR} > 5.6 \times 10^5\ \mathrm{cm}^{-4}$

$$n_{\mathrm{GJ}} = \frac{\Omega \cdot B}{2\pi c(1 - \frac{\Omega R}{c}\sin^2\alpha)}$$

A large number at near LC.

Type I and type II

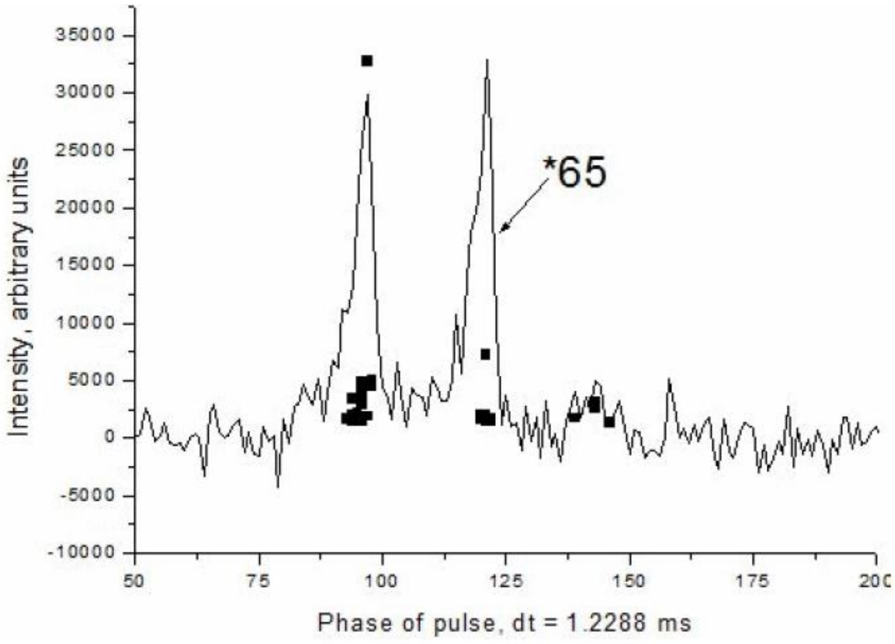

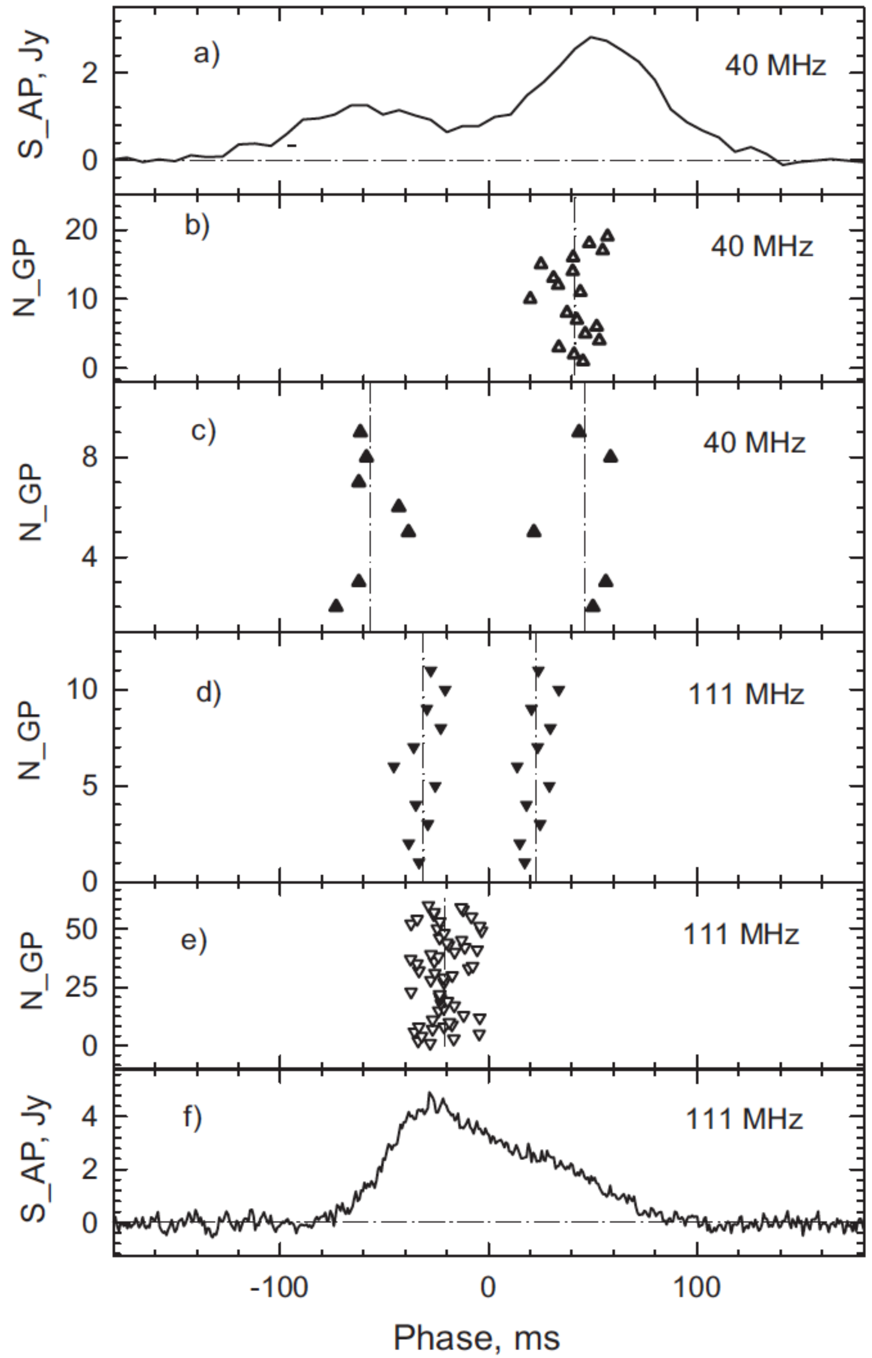

- Kuzmin & Ershov (2004) found that the frequency dependence of the separation of GP emission regions for PSR B0031−07 is similar to that of the width of the AP. This suggests that the type II GPs are emit- ted from a hollow cone over the polar cap instead of LC.

Type I and type II

- Typical timescale of type II GP is several milliseconds while that of type I is micro-second or even nanosecond.
- The maximum flux of type II GP is rarely exceed that of AP by a factor of a thousand.
- Phase of type II GP is stable inside the integrated profile whereas type I GP can occur at phase outside mean pulse profile.

Maybe type II GPs are some bright normal pulses.

GP and FRB

	FRB (the repeater)	GP
Polarization	Strong linear	High linear or circular
Timescale	ms	μs or ns
Luminosity (erg/s)	$10^{41\text{-}44}$	$<10^{39}$
Band structure	-	Zebra pattern
Distribution (power law index)	-1.12	-1.6 to -4.2

$$\frac{L_{\rm FRB}}{L_{\rm GP}} = \frac{S_{\rm FRB} d^2_{\rm FRB}}{S_{\rm GP} d^2_{\rm GP}} \sim 10^5.$$

$$L_{GP} < L_{RP} < L_{FRB}$$

They have different properties among polarization (geometry), timescale (emission scale) and luminosity.

Structures of FRB(e.g., the repeater)

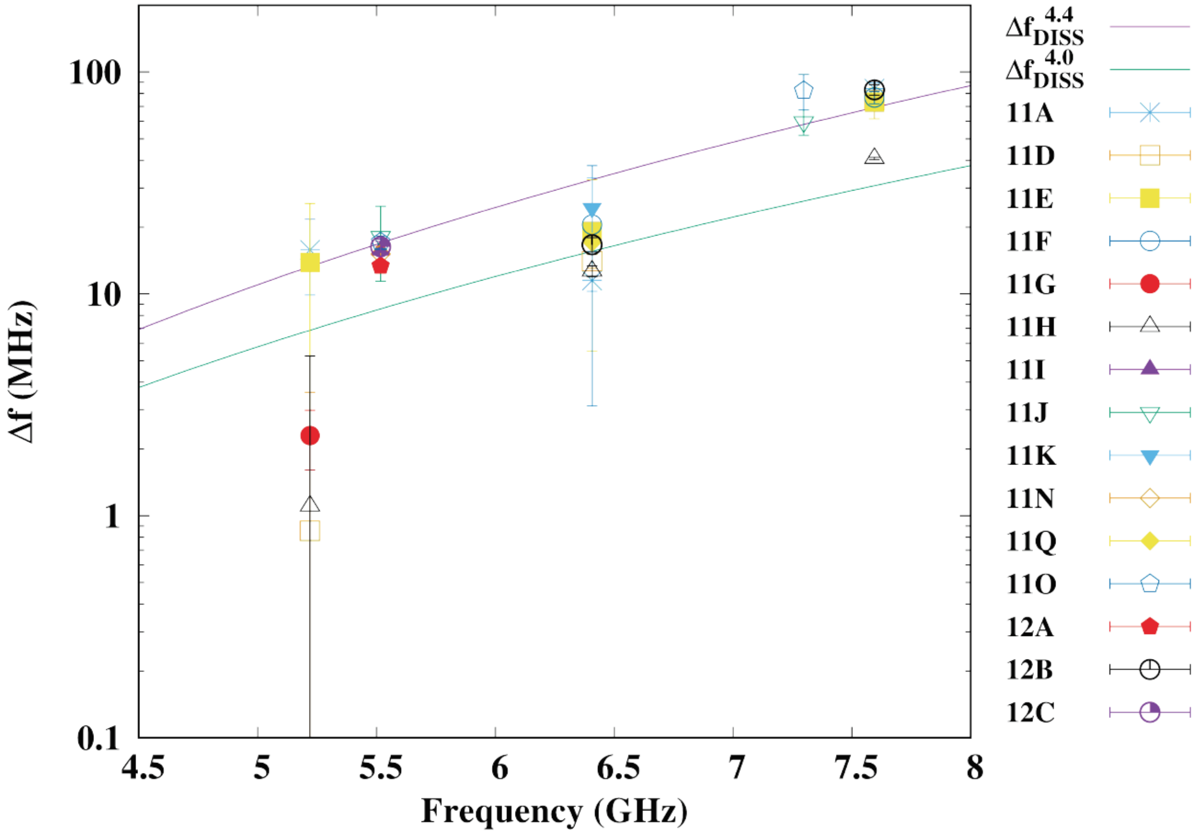

Measured characteristic bandwidth (in MHz) of 15 individual strong bursts of FRB 121102.

Scintillations: $$\Delta f_{\rm DISS} = \frac{1.16}{2\pi\tau_{\rm s}} = \frac{1.16\nu^{[4,4.4]}}{40\pi}\ {\rm MHz}.$$

arXiv:1804.04101

Summary

Thanks!

- We note that the type I GP is originated from the coherent instability of plasma at near LC. The magnetic reconnection could occur at here and accelerate pair plasma injecting into the closed field line region. Since the magnetic mirror like shape of field lines closed to LC, the injected particles may be trapped forming a banana-like emission region.
- The spectrum of the cyclotron-resonant-excited wave shows zebra-pattern-like spectral band structures. These structures can be modulated by the resonance between the cyclotron-resonant-excited wave and back- ground plasma oscillation. The linear band spacing in IP of the Crab pulsar can be well fitted by the model of coherent instability at near LC.
- The modeled density of plasma is $\sim 10^{13-15}\ \mathrm{cm}^{-3}$ with an estimated gradient of $> 5.6 \times 10^{5}\ \mathrm{cm}^{-4}$. Hence, GP is the performance of dense plasma activities at near LC. Similar band structures are expected to be detected in more type I GPs with multi-frequencies.